

## Molecule-Specific Imaging with Mass Spectrometry and a Buckminsterfullerene Probe: Application to Characterizing Solid-Phase Synthesized Combinatorial Libraries

Jiyun Xu,<sup>†</sup> Christopher W. Szakal,<sup>†</sup> Scott E. Martin,<sup>†</sup> Blake R. Peterson,<sup>†</sup>  
Andreas Wucher,<sup>‡</sup> and Nicholas Winograd<sup>\*†</sup>

Contribution from the Department of Chemistry, The Pennsylvania State University,  
University Park, Pennsylvania 16802, and Physics Department, University of Duisburg–Essen,  
45117 Essen, Germany

Received June 6, 2003; E-mail: nxw@psu.edu

**Abstract:** We employ a newly developed buckminsterfullerene (C<sub>60</sub>) primary ion beam with time-of-flight secondary ion mass spectrometry to create molecule-specific images of resin particles employed in the solid-phase synthesis of peptide combinatorial libraries. This new cluster ion source, when operated at an incident energy of 20 keV, is remarkably effective at desorbing small peptides directly from a polymer surface and opens new possibilities for characterizing large arrays of diverse sets of molecules. In addition, the C<sub>60</sub> ion beam may be focused to a spot of 1.5 μm in diameter, enabling molecule-specific images of single 100 μm resin particles to be acquired. We report three significant aspects associated with utilizing the C<sub>60</sub> projectile that show how this technology can be taken to a more advanced level, especially when compared to results obtained with more conventional atomic primary ions. First, the useful yield of molecular ions is generally observed to be enhanced by at least 3 orders of magnitude over those previously possible. Second, the energy dissipation process associated with the C<sub>60</sub> impact is most efficient at desorbing molecules on soft substrates such as polymer surfaces rather than harder substrates such as metals or semiconductors. Third, there is a greatly reduced tendency for insulating surfaces to build up excess charge, obviating the need for charge compensation. Using a small five-member peptide library as a model, we show that by utilizing the focusing properties of the C<sub>60</sub> beam, it is possible to assay the surface composition of 100-μm polymer beads at a rate of up to 10 particles/s. Moreover, even at the picomole level, there are enough sequence ions in the mass spectrum to determine a unique composition. The results illustrate the ability to quickly assay large libraries without the use of tags and suggest the strategy may be applicable to a range of high-throughput experiments.

### Introduction

Arrays of polymer resin particles employed in solid-phase synthesis of combinatorial libraries have proven useful as high-throughput screening templates for drug discovery experiments.<sup>1,2</sup> These templates may contain a million or more different biomolecules in order to cover a significant part of the chemical space associated with a potential drug target.<sup>3</sup> A common approach to assaying these arrays is to identify the chemical nature of each candidate by use of tag molecules, which can be read by a variety of spectroscopic techniques and which are related to the synthetic history of the resin particle.<sup>4–7</sup>

Ligand binding may also be identified by use of fluorescent molecules that are detected by fluorescence microscopy.<sup>4,8–10</sup> Mass spectrometry (MS) offers a more general approach since it is feasible to identify the composition of each member of the array. Electrospray ionization (ESI) and matrix-assisted laser desorption ionization (MALDI) MS techniques have been widely employed in this regard.<sup>11,12</sup>

The above strategies require the molecular array to be characterized in a serial fashion, and hence the throughput is not as high as desired.<sup>13</sup> To improve speed, we have developed a high-throughput protocol that utilizes imaging time-of-flight secondary ion mass spectrometry (ToF–SIMS) to screen high-

<sup>†</sup> The Pennsylvania State University.

<sup>‡</sup> University of Duisburg–Essen.

- (1) Fodor, S. P. A.; Read, J. L.; Pirrung, M. C.; Stryer, L.; Lu, A. T.; Solas, D. *Science* **1991**, *251*, 767–773.
- (2) Lam, K. S.; Salmon, S. E.; Hersh, E. M.; Hruby, V. J.; Kazmierski, W. M.; Knapp, R. J. *Nature* **1991**, *354*, 82–84.
- (3) Bunin, B. A. *The Combinatorial Index*; Academic Press: San Diego, CA, 1998.
- (4) Singh, A.; Yao, Q. W.; Tong, L.; Still, W. C.; Sames, D. *Tetrahedron Lett.* **2000**, *41*, 9601–9605.
- (5) Ohlmeyer, M. H. J.; Swanson, R. N.; Dillard, L. W.; Reader, J. C.; Asouline, G.; Kobayashi, R.; Wigler, M.; Still, W. C. *Proc. Natl. Acad. Sci. U.S.A.* **1993**, *90*, 10922–10926.

- (6) Nestler, H. P.; Bartlett, P. A.; Still, W. C. *J. Org. Chem.* **1994**, *59*, 4723–4724.
- (7) Song, A. M.; Zhang, J. H.; Lebrilla, C. B.; Lam, K. S. *J. Am. Chem. Soc.* **2003**, *125*, 6180–6188.
- (8) McAlpine, S. R.; Schreiber, S. L. *Chem.—Eur. J.* **1999**, *5*, 3528–3532.
- (9) Grondahl, L.; Battersby, B. J.; Bryant, D.; Trau, M. *Langmuir* **2000**, *16*, 9709–9715.
- (10) MacBeath, G.; Schreiber, S. L. *Science* **2000**, *289*, 1760–1763.
- (11) Dawson, P. E.; Fitzgerald, M. C.; Muir, T. W.; Kent, S. B. H. *J. Am. Chem. Soc.* **1997**, *119*, 7917–7927.
- (12) Franz, A. H.; Liu, R. W.; Song, A. M.; Lam, K. S.; Lebrilla, C. B. *J. Comb. Chem.* **2003**, *5*, 125–137.
- (13) Sussmuth, R. D.; Jung, G. *J. Chromatogr. B* **1999**, *725*, 49–65.

density arrays of solid-supported combinatorial libraries.<sup>14</sup> Prior to SIMS analysis, the library is subjected to an appropriate treatment that breaks the chemical bond between the molecules and their polymer support, while retaining the physical location of the analytes. By combining spatial and mass spectral information (mainly molecular ions) acquired in a SIMS image, analysis rates of 10 resin beads/s have been achieved on model systems.<sup>15</sup> This rate is at least an order of magnitude faster than those obtainable with other MS methodologies.<sup>16</sup> With this throughput, it would be possible to completely categorize rather large combinatorial libraries of a million members or more in just a few days.

Previous experiments performed with a Ga<sup>+</sup> primary ion beam have established femtomole sensitivity toward a few small organic compounds with molecular weights less than 300 amu.<sup>17–19</sup> The Ga<sup>+</sup> ion source is selected for its stability and submicrometer imaging resolution, but there are several crucial limitations in the applications to solid-phase synthesized combinatorial chemistry. For Ga<sup>+</sup> ions, the sensitivity and the formation of molecular ions generally drop dramatically with the increase of the molecular weight and the complexity of the analyte.<sup>20</sup> The resulting fragmentation peaks strongly distort the mass spectrum, making structure identification very difficult and even impossible in some cases. The secondary ion yield is further reduced when the target molecules are desorbed from a polymer substrate.<sup>21</sup> Moreover, an insulating polymer substrate such as a polystyrene resin particle may accumulate charge under Ga<sup>+</sup> ion bombardment, causing the complete loss of mass spectral information without the use of proper charge compensation.<sup>22,23</sup> We have been able to improve the situation for Ga<sup>+</sup> ion bombardment to some extent by optimizing a number of empirical parameters in SIMS experiments;<sup>24</sup> however, reliable and accurate characterization of unknown arrays of diverse sets of molecules necessitates the development and usage of a more efficient ion formation method.

It is well-known that heavier projectiles such as Au<sup>+</sup> ions generate a higher yield at higher *m/z* values than lighter projectiles of a similar energy.<sup>25</sup> In addition, molecular dynamics theory suggests that the correlated action of a number of atomic collision cascades below the surface of the solid helps the “lift-off” of large molecules.<sup>26,27</sup> On the basis of these observations, interest has grown in the possible use of polyatomic primary species to enhance the yield even further since multiple cascade

sequences may be generated simultaneously. For example, SF<sub>5</sub><sup>+</sup> ions have been very successful at enhancing the yield of organic ions from polymer thin films.<sup>28,29</sup> Gold cluster ions Au<sub>*n*</sub><sup>+</sup> have also produced large increases in yield for many organic compounds.<sup>30,31</sup> Both sources give rise to very significant increases in secondary ion yield, as compared to atomic projectiles, such as Ar<sup>+</sup>, Xe<sup>+</sup>, Ga<sup>+</sup>, and Cs<sup>+</sup>. The benefits of cooperative effects and the wider and shallower energy deposition resulting from polyatomic projectiles are clearly demonstrated in these experiments.

Here we examine the prospects of utilizing a C<sub>60</sub><sup>+</sup> cluster ion source to speed the assaying of arrays of molecules by use of the SIMS imaging modality. At 10 keV incident energy, the C<sub>60</sub><sup>+</sup> ion beam has been shown to increase the yield of small protein molecules by at least a factor of 1000 relative to Ga<sup>+</sup> for samples prepared as thin films.<sup>32,33</sup> This enhancement is the most dramatic of all the primary ion systems examined to date and is expected to improve even more at higher kinetic energy. Moreover, the C<sub>60</sub><sup>+</sup> ion beam source allows focusing to a 1.5 μm diameter spot with enough current for imaging. In this paper, we report three key advantages of utilizing C<sub>60</sub><sup>+</sup> ion bombardment rather than Ga<sup>+</sup> ion bombardment for assaying combinatorial libraries. First, in contrast to Ga<sup>+</sup> ion bombardment, C<sub>60</sub><sup>+</sup>-induced ion formation from soft and porous polymer substrates is more efficient than from hard substrates such as silicon; second, enhanced secondary ion yields and decreased damage cross sections are measured for peptides desorbed from combinatorial resins with the effect being more pronounced for larger and more complex molecules; and third, due to the high secondary ion yield from polymer surfaces, far less surface charge accumulates on insulating samples. The compatibility of C<sub>60</sub><sup>+</sup> ions with our high-throughput scheme is further explored through the imaging of a five-member peptide library. The C<sub>60</sub><sup>+</sup> ion bombardment experiment on peptides not only produces molecular ions but also generates structurally revealing fragmentation ions as well. This discovery indicates that peptide sequencing is possible for molecules directly attached to the polymer resin. All of these results suggest that imaging SIMS with C<sub>60</sub><sup>+</sup> ion bombardment is particularly suitable for the high-throughput assay of molecular arrays.

## Experimental Section

**Materials.** Sasrin linker–copoly [styrene–1% divinylbenzene (DVB)] resins are purchased from Bioscience Inc (Philadelphia, PA). Rink Amide methylbenzhydrylamine (MBHA) resin (75–150 μm, 0.7 mmol/g) and 9-fluorenylmethoxycarbonyl- (Fmoc-) protected amino acids are purchased from Novabiochem (San Diego, CA). Biotin and other reagents and solvents are obtained from Aldrich (Milwaukee, WI) without further purification. The finder grid is supplied by Ted Pella Inc. (Redding, CA). Silicon {001} wafers (Silicon Quest International Inc, Santa Clara, CA) and poly(tetrafluoroethylene) (Teflon) tapes

- (14) Brummel, C. L.; Lee, I. N. W.; Zhou, Y.; Benkovic, S. J.; Winograd, N. *Science* **1994**, *264*, 399–402.
- (15) Winograd, N.; Braun, R. M. *Spectroscopy* **2001**, *16*, 14–27.
- (16) Shin, Y. G.; van Breemen, R. B. *Biopharm. Drug Disp.* **2001**, *22*, 353–372.
- (17) Braun, R. M.; Beyder, A.; Xu, J. Y.; Wood, M. C.; Ewing, A. G.; Winograd, N. *Anal. Chem.* **1999**, *71*, 3318–3324.
- (18) Enjalbal, C.; Maux, D.; Combarieu, R.; Martinez, J.; Aubagnac, J. L. *J. Comb. Chem.* **2003**, *5*, 102–109.
- (19) Enjalbal, C.; Maux, D.; Subra, G.; Martinez, J.; Combarieu, R.; Aubagnac, J. L. *Tetrahedron Lett.* **1999**, *40*, 6217–6220.
- (20) Diehnelt, C. W.; Van Stipdonk, M. J.; Schweikert, E. A. *Int. J. Mass Spectrom.* **2001**, *207*, 111–122.
- (21) Ruschenschmidt, K.; Schmieders, A.; Benninghoven, A.; Arlinghaus, H. F. *Surf. Sci.* **2003**, *526*, 351–355.
- (22) Gibbons, R.; Dowsett, M. G.; Kelly, J.; Blenkinsopp, P.; Hill, R.; Richards, D.; Loibl, N. *Appl. Surf. Sci.* **2003**, *203*, 343–347.
- (23) Short, R. T.; McMahon, J. M.; Holland, W. M.; Todd, P. J. *J. Am. Soc. Mass Spectrom.* **1994**, *5*, 37–43.
- (24) Xu, J. Y.; Braun, R. M.; Winograd, N. *Anal. Chem.* **2003** (in press).
- (25) Davies, N.; Weibel, D. E.; Blenkinsopp, P.; Lockyer, N.; Hill, R.; Vickerman, J. C. *Appl. Surf. Sci.* **2003**, *203*, 223–227.
- (26) Winograd, N.; Garrison, B. J. *Int. J. Mass Spectrom.* **2001**, *212*, 467–475.
- (27) Taylor, R. S.; Brummel, C. L.; Winograd, N.; Garrison, B. J.; Vickerman, J. C. *Chem. Phys. Lett.* **1995**, *233*, 575–579.

- (28) Gillen, G.; Roberson, S. *Rapid Commun. Mass Spec.* **1998**, *12*, 1303–1312.
- (29) Fuoco, E. R.; Gillen, G.; Wijesundara, M. B. J.; Wallace, W. E.; Hanley, L. J. *Phys. Chem. B* **2001**, *105*, 3950–3956.
- (30) Medvedeva, A.; Wojciechowski, I.; Garrison, B. J. *Appl. Surf. Sci.* **2003**, *203*, 148–151.
- (31) Benguerba, M.; Brunelle, A.; Dellanegra, S.; Depauw, J.; Joret, H.; Lebeyec, Y.; Blain, M. G.; Schweikert, E. A.; Benassayag, G.; Sudraud, P. *Nucl. Instrum. Methods B* **1991**, *62*, 8–22.
- (32) Weibel, D.; Wong, S.; Lockyer, N.; Blenkinsopp, P.; Hill, R.; Vickerman, J. C. *Anal. Chem.* **2003**, *75*, 1754–1764.
- (33) VanStipdonk, M. J.; Harris, R. D.; Schweikert, E. A. *Rapid Commun. Mass Spectrom.* **1996**, *10*, 1987–1991.

(VWR) are cleaned with ethanol (3×), acetone (3×), and hexane (3×) in a sonicator prior to being used as supporting substrates in SIMS experiments.

**Procedure for Coupling Biotin to Sasrin Linker–Copoly (Styrene–1% DVB) Resin.** Sasrin resins (0.05 mmol) were swelled in dichloromethane (DCM) (1 mL) for 30 min. To the resin suspension were then added biotin (24.4 mg, 0.1 mmol, 2 equiv), *N,N'*-dicyclohexylcarbodiimide (DCC) (100 μL, 0.1 mmol, 2 equiv), and catalytic 4-(dimethylamino)pyridine (DMAP) (1.5 mg, 0.25 equiv) in 1 mL of a 1:4 (v/v) mixture of dimethylformamide (DMF)/DCM. After the mixture was stirred at room temperature for several hours, the particles were filtered and washed intensively with DCM (3×), isopropyl alcohol (*i*-PrOH)/DCM (3×), and DCM (6×) and then dried in vacuo. The coupling yield is 70% as determined by weight.

**Procedure for Synthesizing Peptides on Rink Amide MBHA Resin.** Peptide synthesis employed 9-fluorenylmethoxycarbonyl (*N*α-Fmoc) methodology and automated synthesis on an Advanced Chemtech FBS-357 batch-mode synthesizer. Fmoc carbamates on Rink Amide MBHA resin (Novabiochem, 50 mg) were deprotected by the addition of 30% piperidine in DMF (2 × 1 mL for 5 min followed by 1 mL for 20 min). *N*α-Fmoc amino acids (AA) were coupled by the sequential addition of the following reagents in DMF: AA + 1-hydroxybenzotriazole (HOBT, 200 μL, 0.5 M of each component) followed by benzotriazol-1-yloxytris(pyrrolidino)phosphonium hexafluorophosphate (PyBOP, 200 μL, 0.5 M), and diisopropylethylamine (DIEA, 400 μL, 0.5 M). The resin was subsequently shaken at ambient temperature (23 °C) for 30 min. Capping of unreacted amines was achieved by the sequential addition of 30% acetic anhydride in DMF (0.5 mL) and DIEA (0.5 mL, 0.5 M in DMF).

**General Procedure for Vapor-Phase Release of Analyte Molecules.** Because both Sasrin and Rink Amide are acid-labile linkers, vapor-phase trifluoroacetic acid (TFA) is employed to release the analyte molecules from the respective linker. Three milliliters of TFA is placed at the bottom of a 500 mL glass chamber while the resins are held 5 cm above the solvent surface. Since the glass chamber is sealed with Parafilm (VWR), TFA vapor saturates the chamber and reacts with the polymer. The resins are arranged either on a silicon {001} wafer or on PTFE tape for imaging experiments. The typical duration of cleavage varies from 10 min for biotin–Sasrin resin to 20 min for peptide–Rink Amide MBHA resin. Biotin molecules retain their original molecular form after being cleaved from the Sasrin linker. However, the C-termini of respective peptides are converted from COOH groups to CONH<sub>2</sub> groups after being clipped from the Rink Amide linker. This chemistry leads to a decrease of 1 amu in the measured exact mass of the released peptides.

**Ion Beam Current Measurements.** The current induced by the primary ion beam bombardment is measured on the sample holder. However, without use of a Faraday cup, the current measured on surfaces such as flat copper, flat silicon, polymer films, and polymer resins is the sum of current produced by primary ion bombardment, secondary ion emission, and secondary electron emission. To obtain the true values of all these components, for each experiment, we measure the current at the sample under three different conditions: when the holder is grounded, when the holder is biased at +100 V, and when the holder is biased at –100 V. The three current constituents are then calculated from the following equations:

$$\text{at 0 V bias} \quad I_s^0 = I_p + I_- - I_+ \quad (1)$$

$$\text{at +100 V bias} \quad I_s^{+100} = I_p - I_+ \quad (2)$$

$$\text{at –100 V bias} \quad I_s^{-100} = I_p + I_- \quad (3)$$

where  $I_s$  is the current directly measured with a Picoammeter (487, Keithley Instruments, Inc, Cleveland, OH) at the sample at various voltages and  $I_p$ ,  $I_+$ , and  $I_-$  are currents induced by primary ions,

secondary positive ions, and secondary electrons and negative ions, respectively. The true current associated with the number of primary ions hitting the sample is then calculated by combining the sample current measured under the three conditions noted above as

$$I_p = I_s^{+100} + I_s^{-100} - I_s^0 \quad (4)$$

From this result, the currents associated with secondary positive and negative species may be determined as

$$I_+ = I_p - I_s^{+100} \quad (5)$$

$$I_- = I_s^{-100} - I_p \quad (6)$$

This method provides more information than provided by a simple Faraday cup and is useful to judge the relative importance of each component.

**Imaging ToF–SIMS Measurements.** The SIMS instrumentation has been described in detail elsewhere<sup>34</sup> and is briefly discussed below. The instrument is equipped with a Ga<sup>+</sup> liquid metal ion gun (LMIG) and a C<sub>60</sub><sup>+</sup> primary ion source, both of which are directed at the target at a 40° angle relative to the surface normal. Unless otherwise noted, the incident ion dose is kept at or below the static limit of 1 × 10<sup>12</sup> ions/cm<sup>2</sup>. With a repetition rate of 3000 pulses/s, most images are acquired in less than 5 min.

The Ga<sup>+</sup> LMIG is operated at a 15 keV anode voltage. A beam with dc current of several nanoamperes, a spot size of several hundreds of nanometers, and a pulse length of 40 ns can be obtained with a 300 μm beam-defining aperture. To maximize signal intensities from the polymer resins, charge compensation is performed by irradiating the sample with a pulsed beam of 30 eV electrons having a dc current of 1 μA. The electron beam is allowed to strike the sample for 50 μs after each LMIG pulse, during which period the sample stage voltage is held at ground potential.

The C<sub>60</sub><sup>+</sup> primary ion beam system is obtained from Ionoptika Ltd (Southampton, U.K.) and a detailed characterization has been reported recently.<sup>32</sup> The source is operated at an anode voltage of 20 keV. At this primary ion energy, a dc beam current of >3 nA of pure C<sub>60</sub><sup>+</sup> can be obtained at the target by use of a 1000 μm beam-defining aperture, a 2.3 A electron beam filament current, and a 40 V grid voltage. Such conditions give rise to fairly clean mass spectra without major contributions from C<sub>60</sub><sup>2+</sup>, the only other species detectable in the beam. In imaging experiments, we use a 300 μm aperture to achieve better image resolution, and as a result, the total beam current of pure C<sub>60</sub><sup>+</sup> measured at the sample is about 2 nA. The polymer resins examined in this paper do not exhibit charging when analyzed with C<sub>60</sub><sup>+</sup> ions; hence, no charge compensation is performed.

## Results and Discussion

**Imaging Characteristics of C<sub>60</sub><sup>+</sup> Primary Ion Source.** High lateral resolution is a key element of the rapid screening strategy. Due to the size of the emission source, C<sub>60</sub><sup>+</sup> primary ions cannot be as tightly focused as a Ga<sup>+</sup> beam generated from a LMIG tip. The image resolution with C<sub>60</sub><sup>+</sup> ion projectiles is also highly dependent upon the operating specifications. Such effects are illustrated in Figure 1, where four secondary ion microscopy (SIM) images are acquired from the same 200-mesh copper finder grid pressed on indium foil. The 20-keV beam voltage clearly provides better image resolution than the 10-keV beam as shown in Figure 1. Moreover, the smaller beam aperture enhances lateral resolution of an image even though less beam current is available. The best case is pictured in Figure 1d,

(34) Braun, R. M.; Blenkinsopp, P.; Mullock, S. J.; Corlett, C.; Willey, K. F.; Vickerman, J. C.; Winograd, N. *Rapid Commun. Mass Spectrom.* **1998**, *12*, 1246.

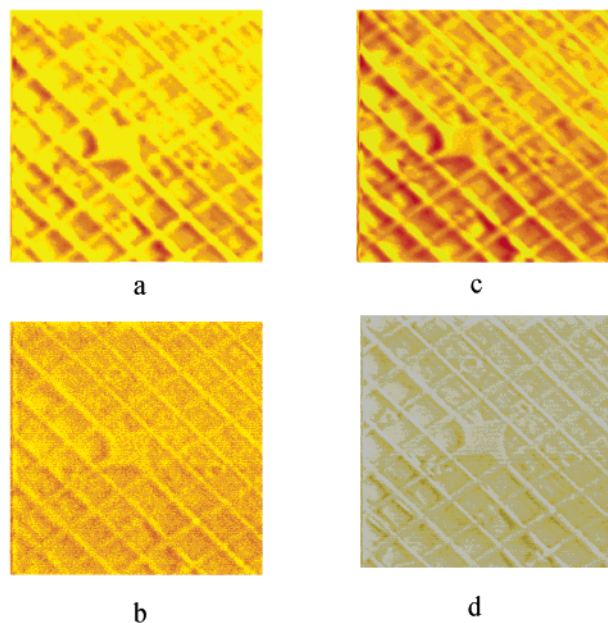


**Figure 1.**  $C_{60}^+$  SEM images of 200 mesh copper grid finder on indium foil obtained with various energies and beam apertures: (a) at 10 keV beam energy and 100  $\mu\text{m}$  beam aperture; (b) at 10 keV beam energy and 30  $\mu\text{m}$  beam aperture; (c) at 20 keV beam energy and 100  $\mu\text{m}$  beam aperture; (d) at 20 keV beam energy and 30  $\mu\text{m}$  beam aperture. All images are 1000  $\mu\text{m}$   $\times$  1000  $\mu\text{m}$ .

obtained with a 20-keV beam utilizing a 30  $\mu\text{m}$  beam aperture. A line scan across the grid features indicates that the lateral resolution is 1.5  $\mu\text{m}$ . The resin particles in our experiments are approximately 100  $\mu\text{m}$  in diameter. To adequately resolve these particles and to achieve an optimal signal-to-noise ratio, all images are acquired with the 300  $\mu\text{m}$  aperture and a pixel density of 128  $\times$  128, resulting in 16 384 individual mass spectra.

**Comparison between  $\text{Ga}^+$  and  $\text{C}_{60}^+$  Ions for Imaging of Combinatorial Resins.** The feasibility of imaging combinatorial resins with  $\text{C}_{60}^+$  ion beams is examined for biotin–Sasrin linker–copoly (styrene–1% DVB) supports. The benefits from switching to  $\text{C}_{60}^+$  from the  $\text{Ga}^+$  primary ion source are also investigated for comparison purposes. Two images of the biotin resin obtained with  $\text{Ga}^+$  and  $\text{C}_{60}^+$  ions are shown in Figure 2. The particles are placed on a silicon {001} wafer and are treated with vapor-phase TFA to break the covalent bond between the biotin molecule and the Sasrin linker prior to mass spectrometry. The panels on the left side of the figure show total ion images presented in a conventional thermal color scale. The panels on the right depict biotin molecular ions denoted in blue and the silicon substrate ions denoted in red. The higher intensities associated with  $\text{C}_{60}^+$  ion bombardment compensate for the relatively large beam diameter and result in image resolution comparable to that found for  $\text{Ga}^+$  ion bombardment. Also interesting to note is that in the total ion image obtained with  $\text{C}_{60}^+$ , the signals originating from the polymer are more intense than those measured from the silicon substrate; however, the opposite is observed in the image obtained with  $\text{Ga}^+$ . This phenomenon indicates that molecular desorption by  $\text{C}_{60}^+$  is most effective with soft and porous substrates rather than hard substrates. This result is in contrast to what is observed for atomic projectiles such as  $\text{Ga}^+$  and  $\text{In}^+$  ions<sup>35</sup> and has been

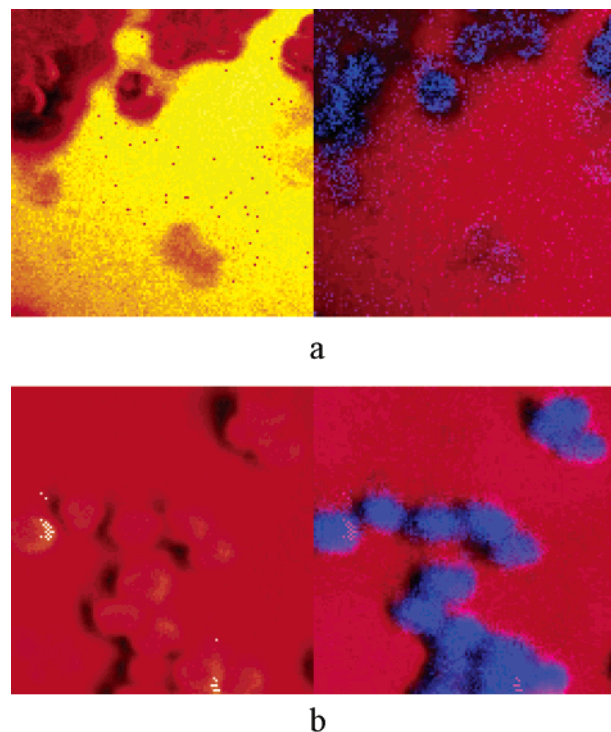


**Figure 2.** SIMS images of Biotin-Sasrin linker–copoly (styrene–1% DVB) resins acquired with  $\text{Ga}^+$  (a) and  $\text{C}_{60}^+$  (b), respectively. The resins are placed on silicon substrate and are examined after biotin molecules are released from the Sasrin linker by vapor-phase TFA. In both panels, the images on the left are total ion images. For the images on the right, the molecular ions of biotin are pictured in blue and silicon substrate ions are pictured in red. Image size: 400  $\mu\text{m}$   $\times$  400  $\mu\text{m}$ .

**Table 1.** Comparison of Biotin Signals Measured with  $\text{Ga}^+$  and  $\text{C}_{60}^+$  from Various Substrates

substrate	secondary ion yield of (M–OH) <sup>+</sup> peak at 227.09 amu (counts/nC)			secondary ion yield of (M+H) <sup>+</sup> peak at 245.10 amu (counts/nC)		
	with $\text{C}_{60}^+$	with $\text{Ga}^+$	$\text{C}_{60}^+/\text{Ga}^+$	with $\text{C}_{60}^+$	with $\text{Ga}^+$	$\text{C}_{60}^+/\text{Ga}^+$
silicon	$2.41 \times 10^7$	$6.79 \times 10^5$	35.5	$1.07 \times 10^7$	$3.12 \times 10^5$	34.3
polymer resin	$1.30 \times 10^6$	$1.17 \times 10^4$	111	$6.86 \times 10^5$	$5.69 \times 10^3$	121

predicted to occur for polyatomic projectiles with computer simulations.<sup>36</sup> Presumably, since each carbon atom in the cluster has 333 eV of kinetic energy, the deposited energy stays closer to the surface, even for these low-density targets.<sup>37</sup>

The signal enhancement capability of  $\text{C}_{60}^+$  is quantitatively illustrated in Table 1. Here, the molecular ion (M+H)<sup>+</sup> and a large fragmentation ion (M–OH)<sup>+</sup> of biotin measured with  $\text{C}_{60}^+$  and  $\text{Ga}^+$  on two samples are compared. The first sample is prepared as a thin film by depositing 5  $\mu\text{L}$  of a water solution of biotin (1 mg/mL) on a silicon {001} wafer, and the second sample is a biotin–Sasrin linker–copoly (styrene–1% DVB) resin after linker cleavage with vapor-phase TFA. Because the quantity and the physical form of the analytes might not be the same, direct comparison between these two samples is not possible. Instead, results from two different ion sources are compared in each case. For both samples, dramatic increases in signal intensities are observed for  $\text{C}_{60}^+$  ion bombardment. In addition, the enhancement exhibits a strong dependence upon

(36) Townes, J. A.; White, A. K.; Wiggins, E. N.; Krantzman, K. D.; Garrison, B. J.; Winograd, N. *J. Phys. Chem. A* **1999**, *103*, 4587–4589.

(37) Postawa, Z.; Czerwinski, B.; Szewczyk, M.; Smiley, E. J.; Winograd, N.; Garrison, B. J. *Anal. Chem.* **2003**, *75*, 4402.

(35) Xu, J. Y.; Braun, R. M.; Winograd, N. *Appl. Surf. Sci.* **2003**, *203*, 201–204.

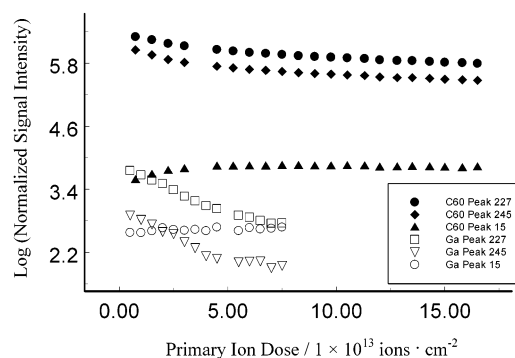


**Figure 3.** Normalized signal intensity as a function of  $C_{60}^+$  or  $Ga^+$  primary ion dose for biotin molecules on polymer resin surfaces. The peaks measured are the  $(M + H)^+$  peak at 245.10 amu, the  $(M - OH)^+$  peak at 227.09 amu, and the reference peak  $CH_3^+$  at 15.02 amu.

the nature of the substrate: about 35-fold more signal is observed when the ions are desorbed from the silicon substrate, while 110-fold more signal is observed when the ions are desorbed from the polymer support. These data complement the data shown in Figure 2 and lead to the conclusion that, unlike  $Ga^+$ ,  $C_{60}^+$  is particularly effective for ion desorption from polymer resin surfaces.

With the establishment of absolute signal intensity for both projectiles, the next goal is to assess their relative secondary ion formation efficiency from polymer resin surfaces. For static SIMS experiments, the efficiency is defined by use of the ion yield relative to the damage cross section. The damage cross section,  $\sigma$ , is defined as the average area damaged per incident particle and is determined by measuring the signal decay of peaks that have a clear structural relationship to the material being sputtered as a function of primary ion dose.<sup>38</sup> In our case,  $\sigma$  resulting from  $C_{60}^+$  or  $Ga^+$  ion bombardment of biotin molecules from polymer resin surfaces is determined by monitoring the signal decrease of the  $(M + H)^+$  peak at 245.10 amu and the associated fragmentation peak  $(M - OH)^+$  at 227.09 amu as shown in Figure 3. It is clear that other than the signal at  $m/z$  15.02 from  $CH_3^+$ , all other peaks decay approximately exponentially with ion dose. However, such decay is much slower for  $C_{60}^+$  ion bombardment and the signal is almost constant for doses up to  $2 \times 10^{14}$  ions/cm<sup>2</sup>. The calculated values of  $\sigma$  for the molecular ion are  $1.5 \times 10^{-14}$  cm<sup>2</sup> for  $Ga^+$  ion bombardment and  $2.3 \times 10^{-15}$  cm<sup>2</sup> for  $C_{60}^+$  ion bombardment. These values are in agreement with data reported by Weibel et al.<sup>32</sup> for similar substrates. Note that by combining the 10-fold smaller value of  $\sigma$  with the 100-fold increase in signal intensity, the efficiency of secondary ion formation, or  $yield/\sigma$ , is increased by 1000-fold.

Sample charging is a common problem when SIMS spectra are recorded from insulating samples. Charge accumulation can occur when there is a net imbalance of primary and secondary ions. If these charges are not neutralized from some other source, the surface potential of the sample can attain values equivalent to the primary ion beam energy. Charge compensation can be performed by irradiating the sample with a pulsed beam of electrons, but adjustment of the electron flux is often difficult, especially for morphologically challenging targets. For our polymer resin particles, charge compensation is required when

**Table 2.** Various Components of the Ion Current Induced by  $Ga^+$  or  $C_{60}^+$  Primary Ion Bombardment on Different Substrates<sup>a</sup>

	substrate	$I_p$ (nA)	$I_e$ (nA)	$I_-$ (nA)	$I_e/I_p$	$I_-/I_p$
$Ga^+$	copper	1.5	1.7	0.60	1.1	0.40
	Teflon	1.5	0.10	0.30	0.066	0.20
$C_{60}^+$	copper	1.3	2.7	1.4	2.1	1.1
	Teflon	1.3	1.6	0.71	1.2	0.55

<sup>a</sup> See text for a definition of the various components of the measured sample current.

**Table 3.** Molecular Species Measured from Two Peptides with  $Ga^+$  and  $C_{60}^+$ , Respectively

	signal intensities of normalized $(M + Na)^+$ peak (counts/nC)	
	Phe-Ala-(Phe) <sub>2</sub> at 552.26 amu	(Phe) <sub>5</sub> at 775.36 amu
$C_{60}^+$	$8.43 \times 10^7$	$1.54 \times 10^7$
$Ga^+$	$3.00 \times 10^3$	0
$C_{60}^+/Ga^+$	$2.81 \times 10^4$	

$Ga^+$  ion bombardment is used but is not required when  $C_{60}^+$  ion bombardment is used, even during high dose conditions. To understand and explain this behavior, the secondary ions and electrons induced by  $Ga^+$  and  $C_{60}^+$  primary ion bombardment at conductive copper surfaces and insulating Teflon surfaces were recorded by the procedure outlined in the Experimental Section. The results are summarized in Table 2. From conductive oxidized copper surfaces, a high yield of secondary ions is produced by both projectiles. In contrast, from insulating Teflon surfaces, the number of secondary ions ejected by  $Ga^+$  ion bombardment is less than a tenth the number of primary ions. For  $C_{60}^+$  ion bombardment, however, the numbers are comparable, leading to more favorable charge balance. This effect is attributed to the high total sputtering yield associated with  $C_{60}^+$  bombardment, which also leads to high secondary ion yields. Even after consideration of the positive charge left by the emission of secondary electrons and negative ions, the net charge accumulated on the surface under  $C_{60}^+$  bombardment is almost zero. Hence, we posit that the high sputtering yield of secondary ions from polymer surfaces offsets the charge carried by the  $C_{60}^+$  primary ions, resulting in no measurable charging.

**Characterization of a Peptide Library with  $C_{60}^+$ .** The advantage of using  $C_{60}^+$  primary ions is particularly striking when one attempts to assay libraries of peptides. Because of the relatively high molecular weights of these biomolecules (generally  $>500$  amu), very small signals are observed with  $Ga^+$  ions. On the other hand, these peptides give rise to substantial molecular ion signals when  $C_{60}^+$  primary ions are employed. Comparisons were carried out for two types of peptides built on Rink Amide MBHA resins. For each type, a solution containing peptides cleaved from a single resin was deposited onto a silicon substrate, followed by  $Ga^+$  and  $C_{60}^+$  ion bombardment. Due to exogenous sources of sodium on silicon, the molecular species detected are the Na adduct of each peptide. As shown in Figure 4 and Table 3, for the peptide Phe-Ala-(Phe)<sub>2</sub> at  $m/z$  529.27, a molecular ion signal enhancement of over 20 000 is observed with  $C_{60}^+$ , with even more enhancements observed for (Phe)<sub>5</sub> at  $m/z$  752.37. Since a single resin bead is loaded with about 1 nmol of peptide, we estimate the limit of detection of  $C_{60}^+$  to these peptides is 1 pmol or better. This improvement in the detection of peptides allows us to

(38) Van Vaeck, L.; Adriaens, A.; Gijbels, R. *Mass Spectrom. Rev.* **1999**, *18*, 1–47.

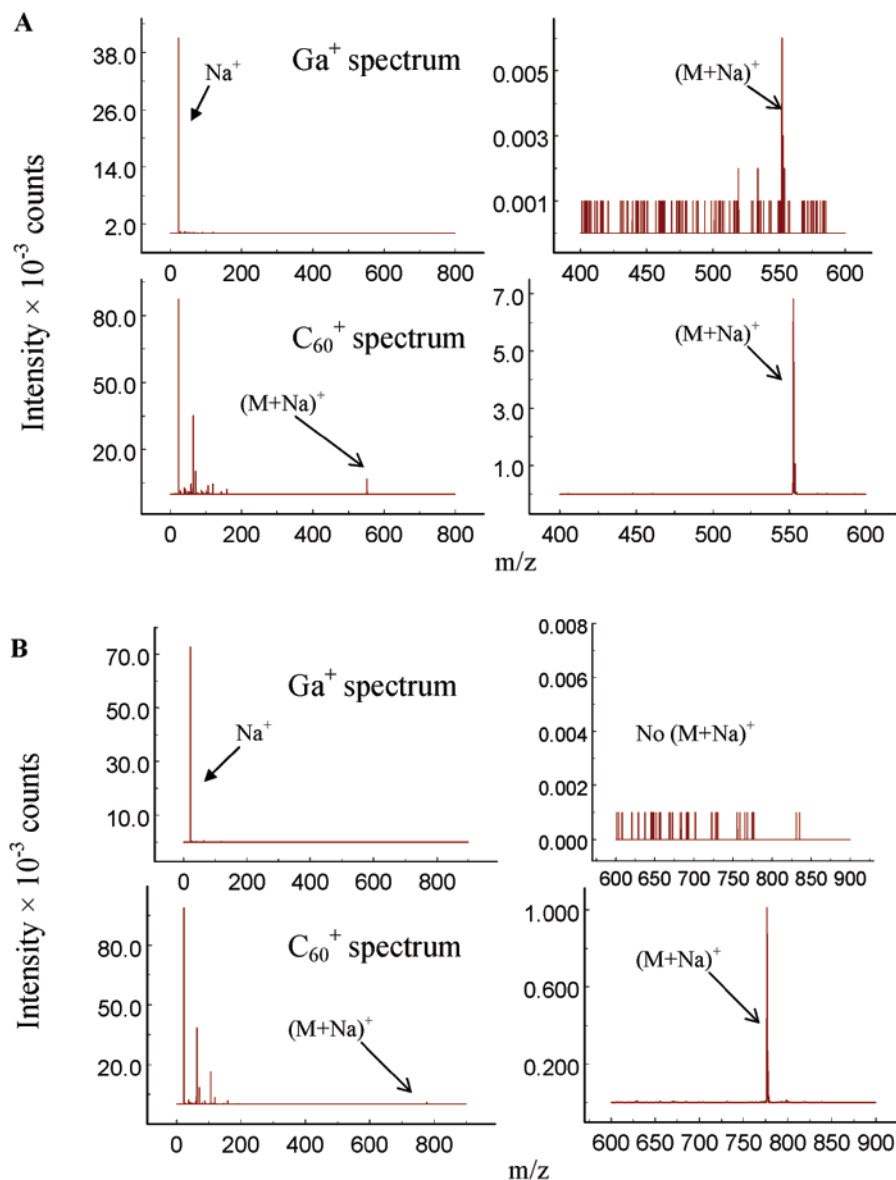


**Figure 4.** Peptide spectra obtained with  $\text{Ga}^+$  and  $\text{C}_{60}^+$  on silicon substrates. (a) Phe-Ala-(Phe)<sub>2</sub> at  $m/z$  529.27 released from Rink Amide MBHA resins in liquid-phase TFA. (b) (Phe)<sub>5</sub> at  $m/z$  752.37 released from Rink Amide MBHA resins in liquid-phase TFA. In both cases,  $\text{Ga}^+$  primary ion dose is  $4.68 \times 10^{11}$  ions/cm<sup>2</sup>;  $\text{C}_{60}^+$  primary ion dose is  $1.56 \times 10^{11}$  ions/cm<sup>2</sup>.

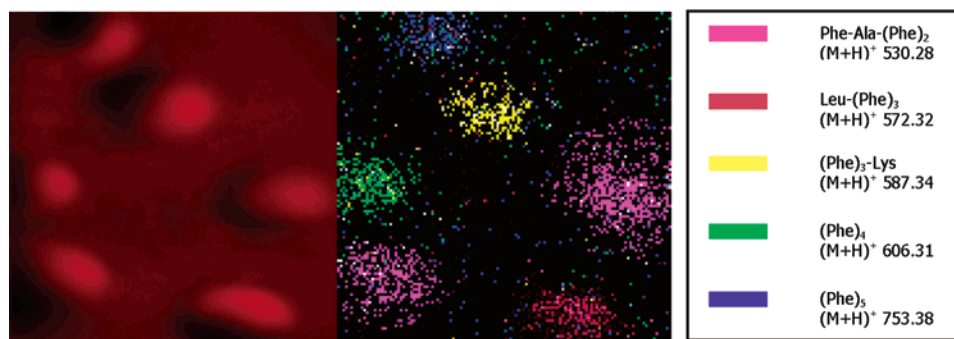


**Figure 5.** SIMS image of six peptide-Rink Amide MBHA resins of five types measured with  $\text{C}_{60}^+$ . The resins are placed on a PTFE substrate. The left panel is a total ion image, and the right panel is color-coded by the index given in the legend. The field of view of this experiment is  $1650 \mu\text{m} \times 1650 \mu\text{m}$ . Primary ion dose is  $1.6 \times 10^9$  ions/cm<sup>2</sup>, well below the static limit.

explore the possibility of high-throughput imaging of combinatorially synthesized peptide libraries by use of  $\text{C}_{60}^+$ .

To test this idea, we examined a model peptide library consisting of five members. The Rink Amide MBHA resins were studied after linker cleavage with vapor-phase TFA. For

this case, the peptides are desorbed from the resin surface which is remarkably free of sodium, and hence they are detected as  $(\text{M} + \text{H})^+$  ions. As shown in Figure 5, the molecular ions of the five peptides are denoted with different colors and it is clear that all of these particles could be readily identified on the basis

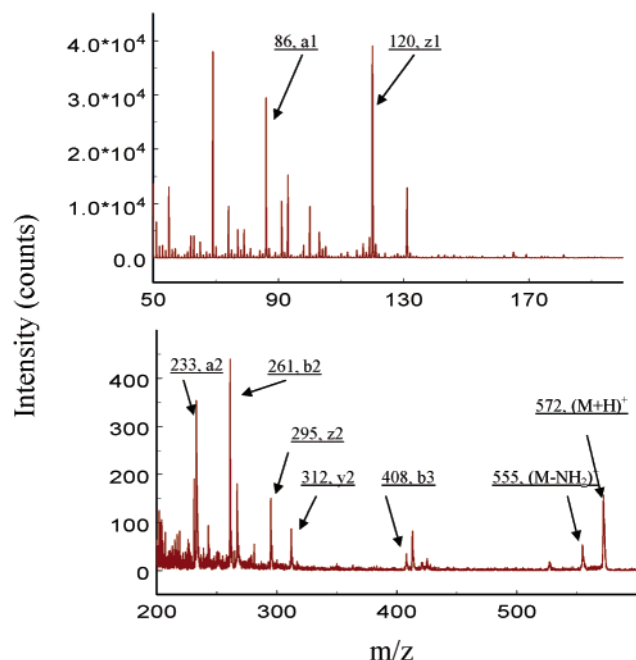


**Figure 6.** SIMS spectrum of solid-phase synthesized Leu-(Phe)<sub>3</sub> measured with C<sub>60</sub><sup>+</sup>. The peptide has been clipped from Rink Amide linker with vapor-phase TFA. The primary ion dose is  $9.2 \times 10^{10}$  ions/cm<sup>2</sup>.

of their spatially distinguishable signals. The analysis rate of this methodology is dependent upon the density and size of the resin array. In our case, the spectrometer has a field of view of about 2 mm  $\times$  2 mm, and the mass spectra may be acquired at the rate of about 10 000/s. With 50  $\mu$ m resin particles, it is possible to create arrays of 10 000 beads/cm<sup>2</sup>. Since it is technically possible to acquire spectra with as few as 100–1000 repetitions, this entire array could be catalogued in less than a few minutes.

The ToF–SIMS spectra acquired by use of C<sub>60</sub><sup>+</sup> projectiles yield fragment ions along with protonated molecular ions that

in most cases either lead directly to an amino acid sequence or provide additional information for structural elucidation. This capability is essential when one attempts to characterize large libraries due to the inevitable appearance of isobaric molecular ions. Currently, collision-induced dissociation (CID) and post source decay (PSD) combined with various ionization techniques including ESI, MALDI, and fast atom bombardment (FAB) are the major strategies for acquiring sequencing information.<sup>39</sup> Nevertheless, compared to imaging SIMS, these methods require more complex sample preparation and offer limited spatial resolution. These factors complicate their use as high-throughput analytical tools for combinatorial chemistry.

An example of the sequencing of Leu-(Phe)<sub>3</sub> from Rink Amide MBHA resins after clipping of the peptide from the linker by vapor-phase TFA is shown in Figure 6. Without application of a matrix or other complex treatments, the resins are directly imaged by use of C<sub>60</sub><sup>+</sup>. The resulting spectrum reveals the molecular ion at  $m/z$  572.32 [(M + H)<sup>+</sup>] along with a series of fragment ions at lower mass. The assignment of all of these peaks is based on a standard nomenclature proposed by Roepstorff and Fohlman,<sup>40</sup> where the N-terminal ions are represented by the symbols a<sub>n</sub>, b<sub>n</sub>, c<sub>n</sub>, and the corresponding C-terminal ions are represented by x<sub>n</sub>, y<sub>n</sub>, and z<sub>n</sub>. The analysis results in the determination of the full sequence of this peptide. Our experiments conducted on several other peptides with varying compositions yield similar sequencing results, suggesting that this observation is not specific to any one peptide. In addition, we notice that the fragmentation pattern can be adjusted by employing more sophisticated sample treatments. More details will be discussed in a subsequent paper.<sup>41</sup>

As shown in Figure 7, the image obtained for Leu-(Phe)<sub>3</sub>, the molecular ions, and the corresponding fragmentation ions are mainly desorbed from the resin particle surface. Hence, there is a simple way to establish the correlation between various mass peaks on the basis of their spatial distribution. If a peak

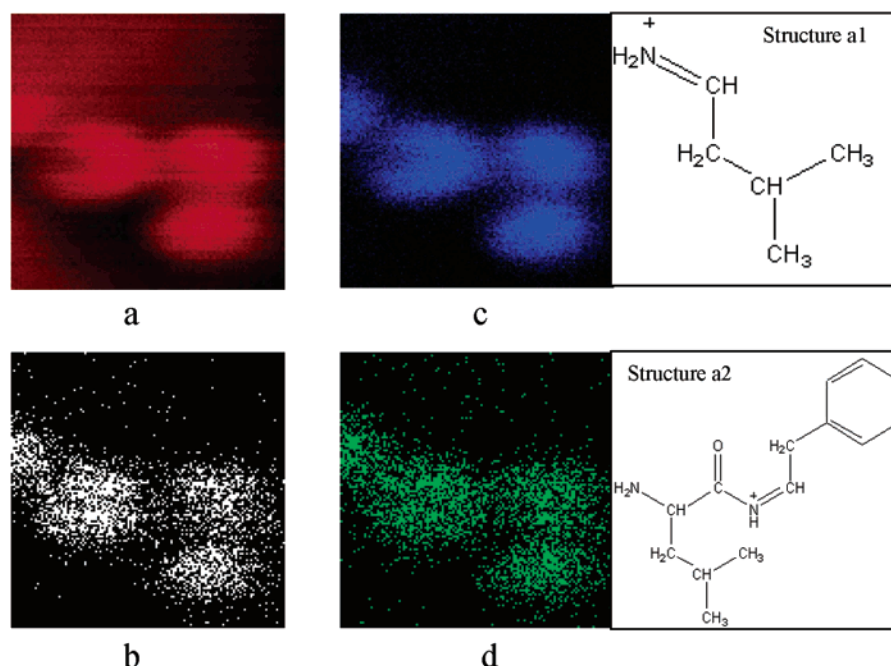


**Figure 7.** SIMS images of Leu-(Phe)<sub>3</sub>-Rink Amide MBHA resins measured with C<sub>60</sub><sup>+</sup>. (a) Total ion image. (b) Molecular ion image. (c) Image of fragmentation peak at  $m/z$  86.10, which corresponds to structure a1. (d) Image of fragmentation peak at  $m/z$  233.17, which corresponds to structure a2. Image size is 450  $\mu$ m  $\times$  450  $\mu$ m.

is not specifically localized on the polymer resin, then in most cases it is not chemically related to the target compound on the resin particle. More importantly, it indicates that direct peptide sequencing and high-throughput analysis can be achieved simultaneously, further adding to the merits of applying  $C_{60}^+$  to the high-throughput characterization of peptide libraries.

### Conclusion

The recently developed  $C_{60}^+$  primary ion beam is a powerful tool in imaging ToF-SIMS for characterizing combinatorial resins. It delivers at least 3 orders of magnitude more efficiency in generating molecular signals from polymer resin surfaces while at the same time reducing the damage resulting from primary ion bombardment when compared to more traditional atomic ion bombardment techniques. The very intense signal measured with  $C_{60}^+$  ions also compensates for the relatively larger beam diameter, resulting in sufficient image resolution for such application. For example, the  $Ga^+$  ion current incident on the sample is about 5 nA at a lateral resolution of 1.5  $\mu m$  but is at least an order of magnitude lower for  $C_{60}^+$  ion bombardment under similar conditions. The quality of all  $C_{60}^+$ -acquired images is nonetheless superior to that obtained for  $Ga^+$  ion bombardment. Moreover, the basic design of the source is well-suited to improvement and we expect to achieve submicrometer lateral resolution soon.

(39) Aebersold, R.; Mann, M. *Nature* **2003**, *422*, 198–207.

(40) Roepstorff, P.; Fohlman, J. *Biomed. Mass Spectrom.* **1984**, *11*, 601.

(41) Xu, J. Y.; Cheng, J.; Winograd, N. *Anal. Chem.* **2004** (in press).

The fact that  $C_{60}^+$  is particularly suitable for analyzing combinatorial resins is reflected in several areas: it desorbs molecules more efficiently from soft and porous substrates such as polymer resins, and it produces a high yield of secondary ions from polymer surfaces, thereby virtually eliminating the charging problem.

The detection limit of  $C_{60}^+$  is not dramatically affected by the molecular weight of the analytes; therefore,  $C_{60}^+$  enables assessment of molecules that are not detectable with  $Ga^+$  due to the lower abundance of signal. We have employed  $C_{60}^+$  to identify one family of such compounds, which are peptides larger than 500 amu with important biological implications, and we discover that the peptides not only are reliably analyzed but also are directly sequenced from their mass spectral fragmentation patterns. More significantly, this application strengthens the efficacy of our high-throughput strategy by achieving many pieces of information at the same time and at a very high rate of speed.

**Acknowledgment.** We thank Professor John Vickerman for pointing out the potential utility of the  $C_{60}^+$  ion source for the assay of combinatorial resins and Juan Cheng for help with sample preparations. Partial financial support was provided by the National Institutes of Health and the National Science Foundation.

JA036549Q